Neutrino-Induced Production of ^{9}Be in Core-Collapse Supernovae

Projjwal Banerjee,[1,*] Yong-Zhong Qian,[2,†] W. C. Haxton,[1,‡] and Alexander Heger[3,§]

[1] *Department of Physics, University of California, and Lawrence Berkeley National Laboratory, Berkeley, CA 94720*

[2] *School of Physics and Astronomy, University of Minnesota, Minneapolis, MN 55455*

[3] *Monash Centre for Astrophysics, School of Mathematical Sciences, Monash University, VIC 3800, Australia*

(Dated: November 27, 2012)

We present two new mechanisms for ν-induced production of ^{9}Be in core-collapse supernovae. In both cases, ν reactions in He shells produce ^{3}H, which then makes ^{7}Li through ^{4}He(^{3}H,γ)^{7}Li. For progenitors of $\sim$8 $M_\odot$, the shocked He-shell material rapidly expands, allowing production of ^{9}Be through ^{7}Li(^{3}H,n_0)^{9}Be. For ultra-metal-poor progenitors of $\sim$11–15 $M_\odot$, neutrons generated by ν reactions in He shells lead to both ^{7}Li$(n,\gamma)^8$Li$(n,\gamma)^9$Li$(e^-\bar{\nu}_e)^9$Be and a rapid neutron-capture process, depending on details of ν spectra, flavor oscillations, and the explosion. We discuss the associated production of ^{7}Li and ^{11}B, related mechanisms for ^{9}Be production that might operate in other sites, and consistency of the identified mechanisms with the observational data.

PACS numbers: 26.30.Jk, 98.35.Bd, 97.60.Bw, 97.10.Tk

It was argued four decades ago that interactions between Galactic cosmic rays (GCRs) and nuclei in the interstellar medium (ISM) could approximately account for the abundances of ^{6}Li, ^{7}Li, ^{9}Be, ^{10}B, and ^{11}B observed in the present Galaxy [1]. Among these isotopes, ^{9}Be has been regarded as special. While big bang nucleosynthesis (BBN) produced an initial abundance of ^{7}Li [2] and the ν process in core-collapse supernovae (CCSNe) may account for much of the Galaxy's current inventory of ^{7}Li and ^{11}B and some fraction of its ^{10}B [3], it is widely accepted that ^{9}Be is produced almost exclusively in the ISM by GCRs (e.g., [4]). In this regard, high-velocity ejecta from very energetic CCSNe can be considered similar to GCRs, though these events may be too rare to generate significant amounts of ^{9}Be in the ISM [5]. Yet recent observations (e.g., [6]) show that there is a linear correlation between log(Be/H) and log(E/H) with a slope $\sim$0.9–1 over $\sim$3 dex, where E stands for O, Mg, Ti, and Fe, all of which are major products of CCSNe. This correlation appears more consistent with primary CCSN production of Be than with production by GCRs only (cf. [4]).

In this letter we present two new mechanisms for CCSN production of ^{9}Be that do not involve interactions with the ISM. The mechanisms are triggered by inelastic interactions of νs from the cooling proto-neutron star (PNS) with nuclei in the He zone of the CCSN progenitor. We calculate this nucleosynthesis with the hydrodynamic code KEPLER [7] using the most recent models of ultra-metal-poor massive progenitors also evolved with this code. For a progenitor of 8.1 $M_\odot$, the He shell, initially at a radius $r \sim 10^9$ cm, is exposed to an intense flux of νs during its expansion following the passage of the shock. Production of ^{9}Be occurs through ^{4}He(^{3}H,γ)^{7}Li(^{3}H,n_0)^{9}Be with ^{3}H made by ν reactions on ^{4}He. For progenitors of 11 and 15 $M_\odot$, it has been shown recently [8] that the charged-current reaction ^{4}He$(\bar{\nu}_e, e^+n)^3$H in outer He shells at $r \sim 10^{10}$ cm produces neutron densities large enough to drive an r-process, the mechanism by which heavy nuclei are synthesized through rapid neutron capture on Fe-group seeds, given a favorable effective $\bar{\nu}_e$ spectrum (see below). We show that a "mini-r process" occurs simultaneously to yield a correlated production of ^{9}Be from ^{7}Li. We explore the sensitivities of the above two mechanisms of ^{9}Be production, as well as the associated ν-process production of ^{7}Li and ^{11}B, to ν emission spectra, flavor oscillations, and the explosion energy. We also discuss similar mechanisms that may produce Be at higher metallicities and implications for chemical evolution of Be and associated elements.

In the updated version of KEPLER, a full reaction network is used to evolve the nuclear composition of a massive star throughout its lifetime and to follow the nucleosynthesis that accompanies the explosion. This includes the nucleosynthesis associated with shock heating of the star's mantle and ν-process nucleosynthesis associated with a ν burst carrying $\sim$300 B ("Bethe"; 1 B = 10^{51} ergs). All ν reactions on ^{4}He are included as in Ref. [8]. The KEPLER progenitors employed here, denoted by u8.1, u11, and u15, have initial metallicities (total mass fraction of elements heavier than He) of $Z = 10^{-4} Z_\odot$ and masses of 8.1, 11, and 15 $M_\odot$ [9]. These models are very similar to earlier ones evolved with a more limited reaction network [10]. The three selected stars develop Fe cores by the end of their evolutions. We simulate an explosion by driving a piston into the collapsing progenitor and following the propagation of the resulting shock wave. We assume that the PNS cools by ν emission according to $L_\nu(t) = L_\nu(0)\exp(-t/\tau_\nu)$, with an initial luminosity per species of $L_\nu(0) = 16.7$ B/s and time constant $\tau_\nu = 3$ s, where $t = 0$ marks the launching

*Electronic address: projjwal@berkeley.edu
†Electronic address: qian@physics.umn.edu
‡Electronic address: haxton@berkeley.edu
§Electronic address: alexander.heger@monash.edu

of the piston. The ν spectra are approximated as Fermi-Dirac distributions with zero chemical potential and fixed temperatures T_{ν_e}, $T_{\bar{\nu}_e}$, and $T_{\nu_x} = T_{\bar{\nu}_x}$ $(x = \mu, \tau)$.

A large set of calculations was performed to assess the sensitivity of the nucleosynthesis to the explosion energy, ν spectra, and flavor oscillations. Numerical CCSN simulations using progenitors similar to u8.1 produce weak explosions with energies of $E_{\rm expl} \sim 0.1\,{\rm B}$ [11], while observations suggest $E_{\rm expl} \sim 1\,{\rm B}$ for more massive progenitors of $\sim$13–20 $M_\odot$ (Fig. 1 of [12]). Below we discuss results for $E_{\rm expl} \sim 0.06$–$0.3\,{\rm B}$ (u8.1 models) and 0.1–1 B (u11/u15 models). Two sets of ν temperatures were used: $(T_{\nu_e}, T_{\bar{\nu}_e}, T_{\nu_x}) = (4, 5.33, 8)\,{\rm MeV}$ (H) and (3,4,6) MeV (S), which represent the harder and softer spectra obtained from earlier (e.g., [13]) and more recent [14] ν transport calculations, respectively. For an inverted ν mass hierarchy, $\bar{\nu}_e \leftrightarrow \bar{\nu}_x$ oscillations occur before νs reach the He shell, which greatly increases the rate of $^4{\rm He}(\bar{\nu}_e, e^+n)^3{\rm H}$ and hence, the neutron density in the outer He shell [8]. We will explore the case of full $\bar{\nu}_e \leftrightarrow \bar{\nu}_x$ interconversion. We label the nucleosynthesis calculations by the progenitor model, the ν spectra, and the explosion energy in units of B, with, e.g., u8.1H.1 indicating progenitor model u8.1, the harder ν spectra H, and $E_{\rm expl} = 0.1\,{\rm B}$. Calculations including $\bar{\nu}_e \leftrightarrow \bar{\nu}_x$ oscillations are denoted by a bar above the H or S. The abundances of ^{28}Si and ^{32}S in the He shells of models u11 and u15 are $\sim$10–30 times larger than those found in the older models of Ref. [10]. Consequently, we also considered modified models u11* and u15* in which the He-shell abundances of ^{28}Si and ^{32}S were reduced to their former values. Representative results for the total mass yields of ^{9}Be, ^{7}Li, ^{11}B, and Fe are given in Table I.

TABLE I: Yields of ^{9}Be, ^{7}Li, ^{11}B, and Fe in $M_\odot$

model	^{9}Be	^{7}Li	^{11}B	Fe
u8.1$\overline{\rm H}$.06	1.57(−10)	2.77(−7)	1.47(−7)	1.89(−3)
u8.1$\overline{\rm H}$.1	1.97(−10)	2.97(−7)	1.35(−7)	1.75(−3)
u8.1H.1	1.20(−10)	2.47(−7)	1.34(−7)	1.79(−3)
u8.1$\overline{\rm S}$.1	5.02(−11)	1.11(−7)	5.67(−8)	1.79(−3)
u8.1S.1	2.55(−11)	8.19(−8)	5.05(−8)	1.80(−3)
u8.1$\overline{\rm H}$.3	2.56(−10)	3.03(−7)	1.06(−7)	1.45(−3)
u11$\overline{\rm H}$.1	1.43(−9)	2.0–2.3(−7)	2.2–8.7(−7)	$<$ 7.73(−2)
u11*$\overline{\rm H}$.1	9.14(−9)	1.5–1.9(−7)	2.6–9.5(−7)	$<$ 7.68(−2)
u11*$\overline{\rm H}$.3	9.81(−10)	3.26(−7)	1.09(−6)	$<$ 8.75(−2)
u15$\overline{\rm H}$.1	$<$ 5.20(−10)	$<$ 3.33(−7)	$<$ 1.34(−6)	$<$ 4.42(−2)
u15*$\overline{\rm H}$.1	$<$ 2.92(−9)	$<$ 3.15(−7)	$<$ 1.36(−6)	$<$ 4.42(−2)
u15*$\overline{\rm H}$.3	7.21(−10)	1.69(−7)	9.50(−7)	$<$ 4.62(−2)

Note: $X(Y) \equiv X \times 10^Y$

Progenitors of $\sim 8\,M_\odot$ have a steeply-falling density profile outside the core and He-shell radii $r \sim 10^9$ cm, in contrast to $\sim 10^{10}$ cm for progenitors of $\gtrsim 11\,M_\odot$. We use Zone 95 in u8.1$\overline{\rm H}$.1 to illustrate ^{9}Be production in such progenitors. Prior to shock arrival, the radius, temperature, and density of this zone are 1.58×10^9 cm, 2.21×10^8 K, and 279 g/cm^3, respectively. The three most abundant nuclei are ^{4}He, ^{12}C, and ^{16}O with initial mass fractions of 0.948, 0.043, and 0.009, respectively. The time evolution of the number fraction Y_i for various nuclei is shown in Fig. 1. Upon being shocked at $t \sim 0.7$ s, Zone 95 reaches a peak temperature of $\sim 8 \times 10^8$ K, so that any ^{9}Be produced previously is burned up. By $t \sim 5$ s the shocked material has expanded and cooled to $\sim 2 \times 10^8$ K, effectively turning off the principal destruction reactions $^9{\rm Be}(p, ^4{\rm He})^6{\rm Li}$ and $^9{\rm Be}(p, d)2^4{\rm He}$. Yet as the material is still close to the PNS and the time still relatively early in units of τ_ν, the flux of νs can efficiently drive the breakup reactions $^4{\rm He}(\nu, \nu' n)^3{\rm He}$, $^4{\rm He}(\nu, \nu' p)^3{\rm H}$, and $^4{\rm He}(\bar{\nu}_e, e^+ n)^3{\rm H}$. Production of ^{9}Be occurs through $^4{\rm He}(^3{\rm H}, \gamma)^7{\rm Li}(^3{\rm H}, n_0)^9{\rm Be}$. Note that ^{9}Be must be produced in the ground state (hence n_0) because all of its excited states are unstable to breakup. We took the rate for $^7{\rm Li}(^3{\rm H}, n_0)^9{\rm Be}$ from Ref. [15].

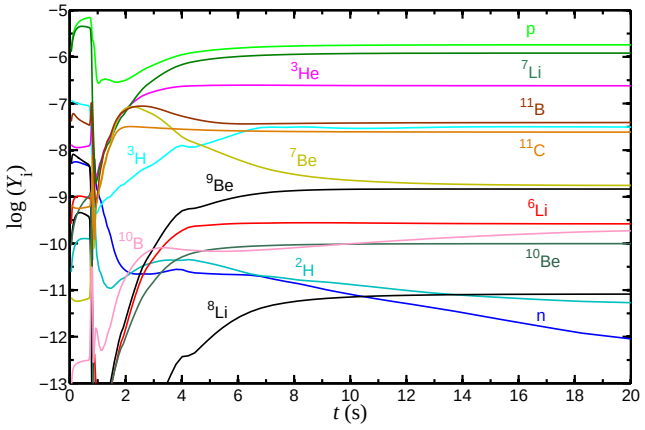

FIG. 1: Time evolution of the number fraction Y_i for various nuclei in Zone 95 of u8.1$\overline{\rm H}$.1.

The yield of ^{9}Be decreases by a factor of $\sim$4 from u8.1$\overline{\rm H}$.1 to u8.1$\overline{\rm S}$.1 (Table I). This reflects the high thresholds of the breakup reactions $^4{\rm He}(\nu, \nu' p)^3{\rm H}$ and $^4{\rm He}(\bar{\nu}_e, e^+ n)^3{\rm H}$, and consequently, their sensitivity to the high-energy tails of the ν spectra. The presence of neutral-current production of ^{3}H reduces the sensitivity to $\bar{\nu}_e \leftrightarrow \bar{\nu}_x$ oscillations: other factors being the same, oscillations increase the yield by up to a factor of $\sim$2. We also explored different explosion energies based on current CCSN models [11]. The change from u8.1$\overline{\rm H}$.1 to u8.1$\overline{\rm H}$.06 (u8.1$\overline{\rm H}$.3) produces a 20% decrease (30% increase) in the ^{9}Be yield primarily through the expansion rate of the shocked He-shell material: a higher $E_{\rm expl}$ results in faster cooling to $\sim 2 \times 10^8$ K and hence, more ^{9}Be. The ^{9}Be production in progenitors like u8.1 depends on the sharply-falling density structure outside the core: the He shell is shocked, expands, and cools on timescales comparable to τ_ν, and thus before the ν flux has diminished significantly. In such progenitors the yield is essentially independent of the initial metallicity.

We choose u11*$\overline{\rm H}$.1 to illustrate the other new mechanism for ν-induced production of ^{9}Be. This model is es-

sentially the same as that used in Ref. [8] to demonstrate a ν-induced r-process in the He shell at low metallicities, a scenario first proposed in Ref. [16] and later explored in Refs. [3, 17]. The importance of $^4\mathrm{He}(\bar{\nu}_e, e^+n)^3\mathrm{H}$ to neutron production and the crucial effect of $\bar{\nu}_e \leftrightarrow \bar{\nu}_x$ oscillations were pointed out in Ref. [8]. Prior to shock arrival, the radius, temperature, and density of Zone 223 in u11*$\overline{\mathrm{H}}$.1 are 1.10×10^{10} cm, 8.49×10^7 K, and 50 g/cm^3, respectively. This zone is composed predominantly of ^{4}He, with ^{12}C at an initial mass fraction of $\sim 10^{-5}$ the second most abundant species. The initial mass fractions of ^{28}Si, ^{32}S, and ^{56}Fe are $\sim 10^{-8}$, 4×10^{-9}, and 4×10^{-8}, respectively. The time evolution of Y_i for various nuclei is shown in Fig. 2.

Neutrons produced mainly by $^4\mathrm{He}(\bar{\nu}_e, e^+n)^3\mathrm{H}$ are captured by Fe-group nuclei to drive an r-process in Zone 223 [8]. An analogous "mini-r process" occurs to produce ^{9}Be through $^7\mathrm{Li}(n,\gamma)^8\mathrm{Li}(n,\gamma)^9\mathrm{Li}(e^-\bar{\nu}_e)^9$Be. The ^{9}Be yield is limited by the short 838 ms half-life of ^{8}Li, which β decays through the 3.0 MeV resonance in ^{8}Be to $^4\mathrm{He} + {}^4\mathrm{He}$, and by the 49.5% branching ratio for ^{9}Li to decay to particle-unstable excited states in ^{9}Be. The above reaction chain operates for $\sim$20 s prior to shock arrival, at which time the temperature and density jump to $\sim 2 \times 10^8$ K and $\sim$220 g/cm^3, respectively, and a short burst of neutrons is released by $^8\mathrm{Li}(^4\mathrm{He}, n)^{11}\mathrm{B}$ (Fig. 2). Over the few seconds, when the postshock temperature stays at $\sim 2 \times 10^8$ K, incomplete destruction of ^{9}Be occurs through $^9\mathrm{Be}(p, {}^4\mathrm{He})^6\mathrm{Li}$ and $^9\mathrm{Be}(p,d)2^4\mathrm{He}$, due to the absorption of protons from $^4\mathrm{He}(\nu, \nu' p)^3\mathrm{H}$ (Fig. 2).

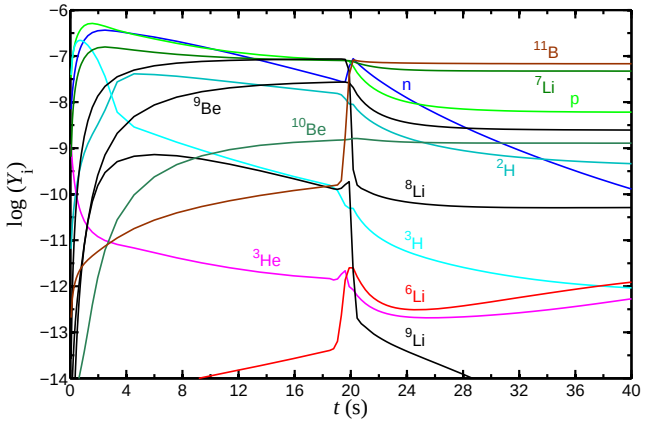

FIG. 2: Time evolution of the number fraction Y_i for various nuclei in Zone 223 of u11*$\overline{\mathrm{H}}$.1.

In contrast to the u8.1 models, the mechanism for the u11/u15 models produces ^{9}Be prior to arrival of the shock and thus is sensitive to the explosion energy (Table I). The higher postshock temperatures found in more energetic explosions greatly enhance ^{9}Be destruction. For $E_{\mathrm{expl}} \gtrsim 1$ B, essentially all of the ^{9}Be made in the He shell prior to shock arrival is destroyed: only that produced in the oxygen shell through $^{12}\mathrm{C}(\nu, \nu')^3\mathrm{He} + {}^9\mathrm{Be}$ [3] survives. The absence of protons and ^{4}He in the oxygen shell eliminates light-particle reactions through which ^{9}Be can be destroyed.

The ^{9}Be yields for the u11/u15 models are also sensitive to the composition of the He shell (Table I). The abundances of the hydrostatic-burning products ^{28}Si and ^{32}S are $\sim$10–30 times higher in u11/u15 than in u11*/u15*. As ^{28}Si and ^{32}S are neutron sinks, Y_n is consequently reduced in u11/u15. The effects on ^{9}Be yields are quadratic in Y_n, as two neutrons are captured to produce ^{9}Be. Increasing the initial metallicity also reduces Y_n due to neutron sinks such as ^{56}Fe. He-shell production of ^{9}Be dominates oxygen-shell production only for initial metallicities of $Z \lesssim 10^{-3} Z_\odot$. A similar bound on He-shell metallicity comes from requiring a neutron density capable of supporting a ν-induced r-process [8]. As in this process, ^{9}Be synthesis requires both hard ν spectra and $\bar{\nu}_e \leftrightarrow \bar{\nu}_x$ oscillations characteristic of an inverted mass hierarchy for ν reactions to produce an adequate Y_n.

In summary, ^{9}Be synthesis in the He zones of models like u11/u15 requires an accompanying r-process and $E_{\mathrm{expl}} \lesssim 0.3$ B. Severe fallback of inner layers was found to occur in all u11/u15 models with $E_{\mathrm{expl}} \lesssim 0.3$ B. Table I thus only gives ranges or upper limits for the yields when production partially or entirely occurs in the fallback zones. The actual yields in these cases depend on the extent of the poorly-understood mixing and ejection associated with fallback.

In the models we explored, ^{9}Be production is accompanied by production of ^{7}Li and ^{11}B (Table I). In all u11/u15 models the latter production operates as described in Ref. [3], through ν breakup of ^{4}He and ^{12}C prior to shock arrival. In contrast, large fractions of ^{7}Li and ^{11}B are produced in u8.1 models by ν interactions occurring in the O-Ne shell that has been severely altered by shock passage. Because this shell is so close ($r \sim 1.8 \times 10^8$ cm) to the core, shock passage leads to complete disassociation of nuclei, which then are reassembled into ^{4}He and Fe-group nuclei as the shell expands and cools. The ν irradiation of this material leads to $^4\mathrm{He}(^3\mathrm{He}, \gamma)^7\mathrm{Be}(^4\mathrm{He}, \gamma)^{11}\mathrm{C}$. The subsequent decay of ^{7}Be and ^{11}C accounts for, e.g., $\sim$70% of the ^{7}Li and $\sim$43% of the ^{11}B produced in u8.1$\overline{\mathrm{H}}$.1. Properties of ^{7}Li and ^{11}B production in all u8.1 models studied include: 1) weak dependence on ν spectra, flavor oscillations, and the explosion energy and no fallback; 2) stable yields within a factor of $\sim$2 of 1.6×10^{-7} and $8.6 \times 10^{-8}\, M_\odot$, respectively; 3) a number-yield ratio $^{11}\mathrm{B}/^7\mathrm{Li}$ of $\sim$0.2–0.4, comparable to the solar value of 0.29 [18] and distinct from the values of $\sim$1–3.6 found in u11/u15 models. The last point is of interest because in the more massive progenitors ^{11}B tends to overwhelm all other yields [3, 19]. For all the models in Table I, production of ^{6}Li and ^{10}B is negligible with $^6\mathrm{Li}/^7\mathrm{Li} \lesssim 10^{-4}$ and $^{10}\mathrm{B}/^{11}\mathrm{B} \sim (0.5\text{–}2) \times 10^{-2}$.

Proposed mechanisms for Be production can be tested against observations. The GCR mechanism (e.g., [4]) is severely constrained by a recent study [6] showing that $[\mathrm{Be/Fe}] \equiv \log(\mathrm{Be/Fe}) - \log(\mathrm{Be/Fe})_\odot \sim 0 \pm 0.5$ for a large sample of stars covering [Fe/H] ~ -3.5 to -0.5. Using

the yields in Table I and the solar abundances in Ref. [18], one obtains [Be/Fe] $\sim 0 \pm 0.2$ for at least three cases: (I) all the u8.1 models with the hard ν emission spectra, (II) u11*$\overline{\text{H}}$.1 with the maximum possible Fe yield, and (III) u11$\overline{\text{H}}$.1, u11*$\overline{\text{H}}$.3, and u15*$\overline{\text{H}}$.3 if their actual Fe yields are $\sim$10% of the upper limits.

Our new Be production mechanisms will be most prominent at low metallicities, when the ISM was enriched on average by a single CCSN. If the ejecta of a CCSN mixes with a total mass of hydrogen of $\sim 10^3 (E_{\rm expl}/0.1\,{\rm B})^{6/7} M_\odot$ [20], one finds [Fe/H] ~ -3.5 to -2.8 (I), -1.4 (II), and -3 to -2.4 (III) for the above cases. The corresponding enrichment of Li is $A({\rm Li}) \equiv \log({\rm Li/H}) + 12 \sim$ 1–1.8. This is well below the level due to BBN and thus consistent with the plateau $A({\rm Li}) \sim 2.2$ observed at these metallicities [2]. Our models also give $A({\rm B}) \sim$ 0.6–1.3, 1.4–1.9, and 1.3–1.9 with B/Be $\sim$ (3–9)$\times 10^2$, 20–85, and 10^2–10^3 in cases I, II, and III, respectively. A small number of data on B exist at [Fe/H] ≤ -1.4, showing $A({\rm B}) \sim$ 0–1.8 but typically with rather low B/Be values of $\sim$10–20 [21]. Large B/Be values have been observed but usually attributed to greater depletion of Be relative to B in stars [21]. Simultaneous observations of Be and B carried out for more stars at [Fe/H] ≤ -1.4 could test this interpretation, versus the intrinsic high yield ratio of B/Be for our models.

In conclusion, we have identified two ν-driven CCSN-associated mechanisms for producing ^{9}Be. The first operates in low-mass, compact progenitors, and is only moderately dependent on ν spectra and flavor oscillations and insensitive to metallicity and the explosion energy. The second mechanism operates in heavier progenitors and requires special conditions: hard ν emission spectra, $\bar{\nu}_e \leftrightarrow \bar{\nu}_x$ oscillations, low metallicities, and low explosion energies. The first three conditions are also those required for a ν-driven r-process to occur in these progenitors. Either mechanism could account for the Be seen in the early Galaxy. The conditions we identified for ^{9}Be synthesis are likely to arise in other astrophysical sites. For example, the merger of two white dwarfs could produce a CCSN similar to the low-mass, compact progenitors studied here (e.g., [22]). In addition, significant ejection of ^{9}Be was found in recent simulations of the merger of two neutron stars (NSs) [23]. It is quite possible that a variety of sources contributed to Be enrichment in the Galaxy, in contrast to exclusive production by GCRs. As Be production may be associated with both the ν-induced r-process at low metallicities ([Fe/H] $\lesssim -3$) and the r-process in NS mergers at higher metallicities (perhaps [Fe/H] $\gtrsim -2.5$), simultaneous observations of Be and r-process elements ought to be pursued.

We thank Stephane Goriely and Thomas Janka for sharing their work on nucleosynthesis in NS mergers. This work was supported in part by the US DOE under de-sc00046548 at Berkeley, DE-AC02-98CH10886 at LBL, and DE-FG02-87ER40328 at UMN, by the NSF under PHY02-16783 through JINA, by ARC Future Fellowship FT120100363 (AH), and by the Alexander von Humboldt Foundation (WCH).

[1] H. Reeves, W. A. Fowler, and F. Hoyle, Nature **226**, 727 (1970); M. Meneguzzi, J. Audouze, and H. Reeves, Astron. Astrophys. **15**, 337 (1971).
[2] See e.g., B. D. Fields, Annu. Rev. Nucl. Part. Sci. **61**, 47 (2011) for a review.
[3] S. E. Woosley, D. H. Hartmann, R. D. Hoffman, and W. C. Haxton, Astrophys. J. **356**, 272 (1990).
[4] N. Prantzos, Astron. Astrophys. **542**, A67 (2012).
[5] B. D. Fields, F. Daigne, M. Cassé, and E. Vangioni-Flam, Astrophys. J. **581**, 389 (2002); K. Nakamura, S. Inoue, S. Wanajo, and T. Shigeyama, Astrophys. J. **643**, L115 (2006).
[6] A. M. Boesgaard, J. A. Rich, E. M. Levesque, and B. P. Bowler, Astrophys. J. **743**, 140 (2011).
[7] T. A. Weaver, G. B. Zimmerman, and S. E. Woosley, Astrophys. J. **225**, 1021 (1978); T. Rauscher, A. Heger, R. D. Hoffman, and S. E. Woosley, Nucl. Phys. A **718**, 463 (2003).
[8] P. Banerjee, W. C. Haxton, and Y.-Z. Qian, Phys. Rev. Lett. **106**, 201104 (2011).
[9] A. Heger, S. E. Woosley, W. Zhang, and C. Joggerst, in preparation (2012).
[10] S. E. Woosley, A. Heger, and T. A. Weaver, Rev. Mod. Phys. **74**, 1015 (2002).
[11] F. S. Kitaura, H.-T. Janka, and W. Hillebrandt, Astron. Astrophys. **450**, 345 (2006).
[12] N. Tominaga, H. Umeda, and K. Nomoto, Astrophys. J. **660**, 516 (2007).
[13] S. E. Woosley, J. R. Wilson, G. J. Mathews, R. D. Hoffman, and B. S. Meyer, Astrophys. J. **433**, 229 (1994).
[14] L. Hüdepohl *et al.*, Phys. Rev. Lett. **104**, 251101 (2010); T. Fischer *et al.*, Astron. Astrophys. **517**, A80 (2010).
[15] C. R. Brune, R. W. Kavanagh, S. E. Kellogg, and T. R. Wang, Phys. Rev. C **43**, 875 (1991); A. Coc *et al.*, Nucl. Phys. A **538**, 515c (1992).
[16] R. I. Epstein, S. A. Colgate, and W. C. Haxton, Phys. Rev. Lett. **61**, 2038 (1988).
[17] D. K. Nadyozhin, I. V. Panov, and S. I. Blinnikov, Astron. Astrophys. **335**, 207 (1998); D. K. Nadyozhin and I. V. Panov, J. Phys. G **35**, 014061 (2008).
[18] K. Lodders, in *Principles and Perspectives in Cosmochemistry*, eds. A. Goswami and B. E. Reddy (Springer, Heidelberg, 2010) 379.
[19] S. M. Austin, A. Heger, and C. Tur, Phys. Rev. Lett. **106**, 152501 (2011).
[20] K. Thornton, M. Gaudlitz, H.-T. Janka, and M. Steinmetz, Astrophys. J. **500**, 95 (1998).
[21] A. M. Boesgaard, E. J. McGrath, D. L. Lambert, and K. Cunha, Astrophys. J. **606**, 306 (2004); K. Tan, J. Shi, and G. Zhao, Astrophys. J. **713**, 458 (2010).
[22] K. J. Shen, L. Bildsten, D. Kasen, and E. Quataert, Astrophys. J. **748**, 35 (2012).
[23] S. Goriely, A. Bauswein, and H.-T. Janka, Astrophys. J. **738**, L32 (2011).